Current Density versus Potential Characteristics of Dye-Sensitized Nanostructured Semiconductor Photoelectrodes. 1. Analytical Expressions

Jae-Joon Lee,[†,§] George M. Coia,[*,‡] and Nathan S. Lewis[*,†]

Noyes Laboratory, 127-72, Division of Chemistry and Chemical Engineering, California Institute of Technology, Pasadena, California 91125, and Department of Chemistry, Portland State University, P.O. Box 751, Portland, Oregon 97207

Received: May 2, 2003; In Final Form: September 25, 2003

A closed-form analytical model is developed to describe the steady-state current density−potential (*J*−*E*) characteristics of dye-sensitized nanostructured semiconductor photoelectrodes. The basic components of the model are a set of differential equations that describe the generation, recombination, and transport of charge carriers in mesoporous semiconductor electrode systems. Charge-carrier transport is treated as a diffusion process, and semiclassical Marcus theory is used to describe the kinetics at the interfaces between the semiconductor and the contacting phase as well as the kinetics at the interfaces with adsorbed dye. The model relates explicitly, within a single formalism, the rate constants for charge transfer of the mesoporous membrane electrode system to conventional intramolecular and intermolecular electron-transfer rate constant expressions and to interfacial electron-transfer processes at planar metal or semiconductor electrodes. The near-equilibrium situation is considered by including the reverse electron-transfer pathways for each rate process of interest. The underlying physical and chemical factors that form the basis of the model are completely parameterized to facilitate input into a numerical simulation algorithm, thereby allowing facile generation of simulated *J*−*E* curves for a wide range of experimental conditions.

I. Introduction

Dye sensitization of wide band gap semiconductors is an important strategy in solar energy conversion research. A major development in this area has been the utilization of photoelectrochemical cells in which the photoanode is a nanostructured mesoporous titanium dioxide membrane supported on a transparent, conductive substrate.[1−6] In this approach, a thin layer of electrolyte containing a dissolved redox mediator is contained between the photoanode and a metal film cathode. The molecular dye species adsorbed onto the mesoporous semiconductor membrane provides spectral sensitization far into the visible, and molecular excited states that form when the dye absorbs light inject electrons into the conduction band of the semiconductor. The injected excess electrons that move through the membrane to the conducting substrate produce a photovoltage and photocurrent in the external circuit and then reduce the oxidized form of the redox couple in the solution phase. The reduced form diffuses back to the photoanode, where it reduces the oxidized dye, regenerating the absorbing state and completing the redox cycle.

The effort to understand this process in greater detail is motivated by both fundamental and applied considerations. Mesoporous semiconductor membranes, like proteins and bilayers, are microheterogeneous environments in which charge separation and transport are not well-understood. On an applied level, elucidation of these processes is a key to optimizing the efficiency of dye-sensitized semiconductor photovoltaics.

* To whom correspondence should be addressed. Phone: +1 503 725 5861. Fax: +1 503 725 3888. E-mail: coia@pdx.edu (GMC). Phone: +1 626 395 6335. Fax: +1 626 795 7487. E-mail: nslewis@caltech.edu (NSL).

† California Institute of Technology.

‡ Portland State University.

§ Current address: Department of Applied Chemistry, Konkuk University, Chungju, Korea.

Over the past decade, increasingly sophisticated models have appeared.[7−13] Of particular importance is the work by Södergren et al., whose model uses one differential equation to describe charge-carrier generation, transport, and recombination.[7]

$$\frac{\partial n}{\partial t} = D_n \frac{\partial^2 n}{\partial x^2} - \frac{n(x) - n_0}{\tau_n} + \Psi_0 \alpha e^{-\alpha x} \qquad (1)$$

In this expression, $n(x)$ is the concentration of electrons at position x in the membrane, n_0 is the electron concentration in the dark, τ_n is the characteristic electron lifetime, and D_n is the diffusion coefficient of the electrons. Equation 1 implies that charge-carrier transport occurs by diffusion and that recombination is a first-order or pseudo-first-order approach to equilibrium.[14]

Steady-state concentration profiles and current density−potential (*J*−*E*) characteristics can be calculated by setting eq 1 equal to zero and solving for n, subject to appropriate boundary conditions. The concentration of electrons at the conducting substrate, $n(0)$, was related to the photovoltage using a Boltzmann-like expression,

$$\frac{n(0)}{n_0} = \exp\left(-\frac{qV}{fk_BT}\right) \qquad (2)$$

where V is the photovoltage, q is the charge on the electron, k_B is the Boltzmann constant, T is the absolute temperature, and f is an ideality factor. Theoretical results were compared to experimentally measured *J*−*E* characteristics and to photocurrent-action spectra. Using the same model, Cao et al. obtained numerical solutions for transient and periodic illumination.[8] Dloczik et al. provided an alternative boundary condition, allowing for kinetically limited extraction of electrons from the

10.1021/jp035194u CCC: $27.50 © 2004 American Chemical Society
Published on Web 04/08/2004

mesoporous semiconductor membrane to the substrate instead of the diffusion-controlled extraction implied by eq 2.[9] Various other approaches have also been taken to model the $J-E$ characteristics of solar cells based on such nanocrystalline semiconductors.[10−12]

A fundamentally different model was subsequently proposed by Shwarzburg et al.[13] These authors emphasized the importance of the junction potential between the semiconductor membrane and the conducting substrate in promoting charge separation and in controlling the photovoltage. To test the validity of this model, Pichot et al. measured the open-circuit photovoltages of dye-sensitized TiO_2 membranes deposited on substrates having dissimilar work functions.[15] The model could not be easily reconciled with these results or with recent electrochemical impedance measurements.[16]

At present, the greater share of experimental agreement[17] appears to lie with the models represented by eqs 1 and 2. Despite its utility, this model in its current formulation relies on several assumptions that limit its applicability.[18] The present study was undertaken in order to generalize the model, making it applicable to a broader range of experimental and hypothetical conditions. These situations include cases in which the injection or regeneration efficiency is not unity, recombination is not first-order in electrons,[19,20] diffusion of the charge carriers is much faster or much slower than that in the prototypical device, or drift and diffusion both contribute to mass transport. Many such examples can be found in the recent literature, and more can be anticipated on the basis of the continuing effort to improve the efficiency and stability of dye-sensitized mesoporous photoelectrodes. In this paper, we describe an extensive mathematical model for light harvesting, charge separation, charge transport, recombination, and electrolyte reduction reactions in such photoelectrochemical cells.

II. Theory

A. Basic Reaction Schemes. Electrons and holes, having the concentrations n and p, respectively, can exist in any of three regions: the semiconductor phase (s), the interfacial region containing the adsorbed sensitizer (d), and the contacting phase (c). Because it is unlikely that both charge carriers will accumulate in semiconductors being sensitized by a single dye, in systems where the concentration of electrons in the semiconductor (n_s) is significant, it is generally not necessary to consider holes in the semiconductor (p_s), and vice versa. In the following derivations, we will assume that the electron is the charge carrier in the semiconductor, with the opposite case readily described by exchange of the symbols n and p throughout.

Scheme 1 depicts a general reaction treatment of the dynamics of such systems. Although not explicitly indicated, a reverse reaction pathway also exists for each of the electron-transfer pathways indicated in the scheme. The reverse rate constants for each process, along with the relevant equilibrium constants, are required in the kinetics model for generality and to describe specifically situations in which some of the chemical reactions take place near thermodynamic equilibrium. For convenience, the rate equations for the situation far from equilibrium are considered first, and then the equilibrium situation will be discussed in conjunction with the actual charge-transfer model and resultant rate expressions.

The excited sensitizer (d^*) can be quenched either oxidatively (case O) or reductively (case R). Pathways on the left portion of Scheme 1 are relevant for strategy R, while pathways on the right are relevant for strategy O. Though all of the possible

SCHEME 1: Dye-Sensitization Kinetics for the Case Where the Electron Is the Charge Carrier in the Semiconductor[a]

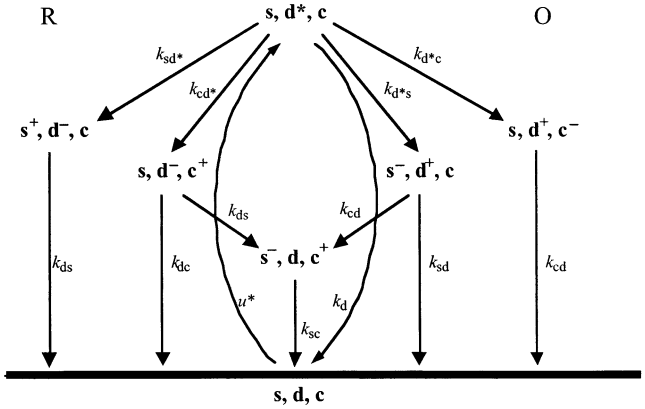

[a] The labels R and O refer to reductive and oxidative quenching of the sensitizer, respectively.

quenching pathways are represented in Scheme 1, there is apparently no system at present for which it is necessary to consider both the left and right parts simultaneously. Hence, only the situation in which one of these processes is dominant is discussed further below.

Either case O or case R involves five kinetically significant species: the excited sensitizer (d^*) and four different charge carriers. If u_i denotes the rate at which species i is formed (or destroyed) by chemical reaction, and if the rate of formation of the excited sensitizer is denoted as u^*, for case R one obtains

$$u_{d^*} = u^* - d^*(k_{sd^*}n_s + k_{cd^*}n_c + k_d) \tag{3.1}$$

$$u_{n_s} = -k_{sd^*}n_s d^* + k_{ds}n_d - k_{sc}n_s p_c \tag{3.2}$$

$$u_{n_d} = d^*(k_{sd^*}n_s + k_{cd^*}n_c) - n_d(k_{ds} + k_{dc}p_c) \tag{3.3}$$

$$u_{p_c} = -u_{n_c} = k_{cd^*}n_c d^* - k_{dc}n_d p_c - k_{sc}n_s p_c \tag{3.4}$$

For case O

$$u_{d^*} = u^* - d^*(k_{d^*c}p_c + k_{d^*s} + k_d) \tag{4.1}$$

$$u_{n_s} = k_{d^*s}d^* - k_{sd}n_s p_d - k_{sc}n_s p_c \tag{4.2}$$

$$u_{p_d} = d^*(k_{d^*s} + k_{d^*c}p_c) - p_d(k_{sd}n_s + k_{cd}n_c) \tag{4.3}$$

$$u_{p_c} = -u_{n_c} = -k_{d^*c}p_c d^* + k_{cd}n_c p_d - k_{sc}n_s p_c \tag{4.4}$$

The overall rate (u_i) of each process has units of flux, inverse square centimeters inverse seconds. The concentrations of charge carriers in the contacting phase (p_c and n_c) are given in inverse cubic centimeters, while the different forms of dye species (d, d^*, and p_d) are represented by surface concentrations, having units of inverse square centimeters. These rate equations are subject to the additional constraint that the total concentration of dye species must be equal to d_0, the analytical concentration of the dye:

$$d + p_d + d^* = d_0 \tag{5}$$

Dye-sensitization of most operational solar cells usually proceeds by quenching of the excited sensitizer by injection into the semiconductor (case O in Scheme 1), so we now focus

SCHEME 2: Energy Diagram and the Associated Interfacial Electron-Transfer Rate Constants at the Dye-Sensitized Nanocrystalline TiO_2/Electrolyte Interface

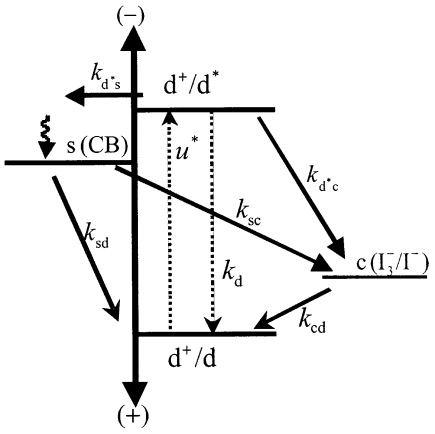

on a system of particular interest, dye-sensitization according to case O, as described in the simplified energetic and kinetics diagram of Scheme 2. Optical excitation of the dye (u^*) gives rise to an injection (k_{d^*s}) into the conduction band of TiO_2. The excited state can also either thermally decay (k_d) to the ground state or be quenched by electron transfer to oxidized species in the electrolyte solution (k_{d^*c}). The oxidized dye cation is reduced by the redox species present in the electrolyte (k_{cd}) (regeneration). Electron transfer from the photoinjected electrons in the conduction band of the semiconductor to the dye cation (k_{sd}) (recombination) competes with reduction of the dye by species in the electrolyte solution. Other electron-transfer processes, which produce cathodic currents that oppose the photocurrent, include the reaction between electrons in the membrane and oxidized redox species in the electrolyte (k_{sc}) (direct reduction) and the reaction between electrons in the conducting substrate and the electrolyte (k_{oc}) (the leakage current; not shown in this scheme).

B. Modified Kinetics Equations for Systems That Use the Iodide/Triiodide Redox Couple and for Reversible Rate Processes in the Cell. Because the redox couple in the most efficient dye-sensitized cells to date is the I_3^-/I^- system, the basic kinetics equations presented above require modification to encompass the situation in which the kinetically important electron-transfer species are not the predominant chemical components or charge carriers in the electrolyte. For example, in one mechanistic possibility, the overall reaction mechanism for the oxidation and reduction of I_3^-/I^- solutions can be broken down into a series of successive reactions:[10,19,21,22]

$$I_3^- \overset{K_1}{\rightleftharpoons} I_2 + I^- \tag{6.1}$$

$$I_2 \overset{K_2}{\rightleftharpoons} 2I^\bullet \tag{6.2}$$

$$I^\bullet + e \xrightarrow{k_{et}} I^- \tag{6.3}$$

where reactions 6.1 and 6.2 are fast chemical reactions, which are assumed to be always in equilibrium.[22] In this mechanism, triiodide (I_3^-) is the oxidized species in the overall reaction and is the charge carrier in the contacting phase, but it is not the oxidized species in the elementary single-electron-transfer process. The concentration of elementary iodine atoms ([I]) can be related to the concentration of the actual charge carriers in the contacting phase by

$$[I] = \sqrt{K_I \frac{p_c}{n_c}} \tag{7}$$

where $K_I = K_1K_2$ and n_c and p_c are the concentrations of the charge carriers, that is, iodide ($[I^-] = n_c$) and triiodide ($[I_3^-] = p_c$), respectively. Thus, with no loss of generality, the kinetics equations can readily be modified to account for the situation in which the predominant chemical species is not the one involved in the rate-determining electron-transfer kinetics processes of interest, with the specific expression of eq 7 applicable to the mechanism represented in eqs 6.1−6.3.

It is of interest to describe the situation in which at least some of the chemical reactions are near equilibrium. The reverse rates for these reaction steps can be included mathematically by incorporation of a reversibility factor (R factor, R_{ij}) for each process of interest, where R_{ij} is a numeric value between zero and unity that represents the degree of reversibility of each process of interest. A general procedure to include the reverse pathways is described in Appendix I, along with the definition of the R factors for each of the individual electron-transfer processes (R_{ij}) shown in the set of equations below. Specific definitions of the R factors, R_{ij}, used in the present treatment are listed in Table 1.

Modifying the basic kinetics rate equations, eqs 4.1−4.4, to include the kinetics of the I_3^-/I^- system described above, and incorporating reversibility through the R factors, yields:

$$u_{d^*} = u^* - d^*\left\{k_{d^*c}\sqrt{K_I\frac{p_c}{n_c}} + k_d + k_{d^*s}(1 - R_{d^*s})\right\} \tag{8.1}$$

$$u_{n_s} = k_{d^*s}d^*(1 - R_{d^*s}) - k_{sd}n_sp_d(1 - R_{sd}) - k_{sc}n_s\sqrt{K_I\frac{p_c}{n_c}}(1 - R_{sc}) \tag{8.2}$$

$$u_{p_d} = d^*\left\{k_{d^*s}(1 - R_{d^*s}) + k_{d^*c}\sqrt{K_I\frac{p_c}{n_c}}\right\} - p_d\{k_{sd}n_s(1 - R_{sd}) + k_{cd}n_c(1 - R_{cd})\} \tag{8.3}$$

$$u_{p_c} = -u_{n_c} = -k_{d^*c}d^*\sqrt{K_I\frac{p_c}{n_c}} + k_{cd}n_cp_d(1 - R_{cd}) - k_{sc}n_s\sqrt{K_I\frac{p_c}{n_c}}(1 - R_{sc}) \tag{8.4}$$

C. Expressions for Interfacial Charge-Transfer Rate Constants. The rate constant expression for interfacial electron-transfer at the electrode/electrolyte interface has been discussed recently on the basis of the Marcus electron-transfer theory of nonadiabatic processes.[23] The rate constants can be expressed as a function of three fundamental parameters for the species involved in each reaction of interest: the electronic coupling matrix element (H_{AB}), the standard free energy change ($\Delta G^{\circ\prime}$), and the reorganization energy (λ).[24]

The same formalism can be extended to describe electron-transfer rate constants at the interfaces between the semiconductor nanoparticles and the contacting electrolyte solution. However, unlike the case at conventional bulk semiconductor/electrolyte interfaces, an individual nanoparticle cannot develop sufficient space charge to support a potential drop across the

TABLE 1: Summary of the Kinetics Rate Constants, *R* Factors, and Free Energy Changes $\Delta G_{ij}^{\circ\prime}$ (E=0)

ij	rate constants (k_{ij})		R_{ij}		$\Delta G_{ij}^{\circ\prime}$ (E=0)
d^*s (1/s)	$k_{d^*s}(E) = \frac{2\pi}{\hbar}\frac{1}{\sqrt{4\pi\lambda_{d^*s}kT}}\lvert H_{d^*s}\rvert^2\rho_{\mathrm{TiO_2,eff}}I(\lambda_{d^*s},E)$	(K.1.1)	$qE^{\circ}(d^{*+}/d^*) - \mathbf{E}$ ($\mathbf{E} < \mathbf{E}_{cb}$) (R.1)		$qE^{\circ\prime}(d^{*+}/d^*) - \mathbf{E}$ ($\mathbf{E} < \mathbf{E}_{cb}$) (G.1)
	$I(\lambda_{d^*s},E) = \int_{E_{cb}}^{-\infty}\{1 - F(\mathbf{E},E)\}\exp\left\{-\frac{[\Delta G_{d^*s}^{\circ\prime}(\mathbf{E}) + \lambda_{d^*s}]^2}{4\lambda_{d^*s}kT}\right\}\mathrm{d}\mathbf{E}$	(K.1.2)			
sd (cm^3/s)	$k_{sd} = \frac{2\pi}{\hbar}\frac{1}{\sqrt{4\pi\lambda_{sd}k_BT}}\lvert H_{sd}\rvert^2\frac{l_{\mathrm{TiO_2}}}{d_{\mathrm{TiO_2}}^{2/3}(6/\pi)^{1/3}}\exp\left[-\frac{[\Delta G_{sd}^{\circ\prime} + \lambda_{sd}]^2}{4\lambda_{sd}k_BT}\right]$	(K.2)	$\frac{1}{K_{sd}}\frac{(d_0/p_d - 1)}{n_s}$	(R.2)	$\mathbf{E}_{cb} - qE^{\circ\prime}(d^+/d)$ (G.2)
sc (cm^4/s)	$k_{sc} = \frac{2\pi}{\hbar}\frac{1}{\sqrt{4\pi\lambda_{sc}kT}}\frac{l_{\mathrm{TiO_2}}}{d_{\mathrm{TiO_2}}^{2/3}(6/\pi)^{1/3}}\lvert H_{sc}^{\circ}\rvert^2\{\beta_{sc}^{-1}\}\exp\left[-\frac{[\Delta G_{sc}^{\circ\prime} + \lambda_{sc}]^2}{4\lambda_{sc}kT}\right]$	(K.3)	$\frac{1}{K_{sc}(K_I)^{1/2}}\sqrt{\frac{n_c}{p_c}}\frac{n_c}{n_s}$	(R.3)	$\mathbf{E}_{cb} - qE^{\circ\prime}(\mathrm{I/I^-})$ (G.3)
cd (cm^3/s)	$k_{cd} = \frac{2\pi}{\hbar}\frac{1}{\sqrt{4\pi\lambda_{cd}k_BT}}\lvert H_{cd}^{\circ}\rvert^2\{2\pi R^2\beta^{-1}\}\exp\left[-\frac{(\Delta G_{cd}^{\circ\prime} + \lambda_{cd})^2}{4\lambda_{cd}k_BT}\right]$	(K.4)	$\frac{(K_I)^{1/2}}{K_{cd}}\sqrt{\frac{p_c}{n_c}}\frac{(d_0/p_d - 1)}{n_c}$	(R.4)	$qE^{\circ\prime}(\mathrm{I/I^-}) - qE^{\circ\prime}(d^+/d)$ (G.4)
d^*c (cm^3/s)	$k_{d^*c} = \frac{2\pi}{\hbar}\frac{1}{\sqrt{4\pi\lambda_{d^*c}k_BT}}\lvert H_{d^*c}^{\circ}\rvert^2\{2\pi R^2\beta^{-1}\}\exp\left[-\frac{(\Delta G_{d^*c}^{\circ\prime} + \lambda_{d^*c})^2}{4\lambda_{d^*c}k_BT}\right]$	(K.5)	n/a[a]		$qE^{\circ\prime}(d^{*+}/d^*) - qE^{\circ\prime}(\mathrm{I/I^-})$ (G.5)
oc (cm/s)	$k_{oc}(E) = \frac{2\pi}{\hbar}\frac{1}{4\pi\lambda_{oc}kT}\lvert H_{oc}^{\circ}\rvert^2\frac{1}{\beta}\rho_{\mathrm{SnO_2,eff}}I(\lambda_{oc},E)$	(K.6.1)	n/a		$\mathbf{E} - \boldsymbol{qE}^{\circ\prime}(\mathrm{I/I^-})$ (G.6)
	$I(\lambda,E) = \int_{-\infty}^{\infty}F(\mathbf{E},E)\exp\left\{-\frac{[\Delta G_{oc}^{\circ\prime}(\mathbf{E}) + \lambda_{oc}]^2}{4\lambda_{oc}kT}\right\}\mathrm{d}\mathbf{E}$	(K.6.2)			

[a] Not applicable.

nanoparticle. Additionally, due to the highly insulating nature of TiO_2 nanoparticles and the screening effect caused by electrolyte permeation into the nanoporous membrane, an applied potential is largely screened from the processes occurring at the interfaces between the electrolyte and the particles of the semiconductor membrane. Hence, except for the very small fraction of particles that are not effectively screened by the electrolyte, the dependence of the interfacial rate constants at the nanoparticle/electrolyte interfaces on the potential applied to the current-collecting contact can be neglected. The resulting rate constant expressions, which can be used as input parameters to the model of interest, are presented in Table 1.

In these rate constant expressions, $\hbar$ is Plank's constant divided by 2π, l_{sc} is the effective coupling length of the redox acceptor wave function into the semiconductor, d_{sc} is the atomic density of the semiconductor ($sc = TiO_2$),[23] $|H_{ij}|^2$ is the square of the electronic coupling matrix element at a given distance, $\rho_{m,\mathrm{eff}}$ ($m = TiO_2$, SnO_2) is the effective density of states in the substrate that couple to the electron-transfer process, and $F(\mathbf{E},E)$ is the Fermi occupancy function in the solid as a function of energy $\mathbf{E}$ at the potential extended to the system of interest, E:

$$F(\mathbf{E},E) = \frac{1}{1 + \mathrm{e}^{\{qE + \mathbf{E}(A/A^-) - \mathbf{E}\}/kT}} \qquad (9)$$

The appearance of an attenuation factor (β) in eqs K.3−K.5 (Table 1) represents the results of integrating the electronic coupling term, $|H_{ij}(r)|^2 = |H_{ij}^{\circ}|^2\exp\{-\beta(r - r_0)^2$, with respect to r, to account for the random distribution of redox species in the electrolyte. Table 1 also presents expressions for the driving force, ΔG_{ij}°, of each rate process in terms of key thermodynamic properties of the system.

The rate constants for the regeneration (k_{cd}) and quenching of the dye excited states by species in the electrolyte (k_{d^*c}) are not of precisely the same form as those for electron transfer at the electrode/electrolyte interface.[24] These rate constants can however be obtained by adapting the semiclassical Marcus treatment of donor−acceptor type homogeneous electron-transfer reactions and by integrating over all possible reactant pairs.[25] The values of R in eqs K.4 and K.5 (in Table 1) represent the sum of the radii of the reactants, each being treated as spherical, and λ_{cd} and λ_{d^*c} are defined as the sum of the reorganization energies of the donor and acceptor for the reaction of interest. A steric factor is also needed to account for the fact that only a portion of the adsorbed sensitizer is accessible for collisions with the species in the electrolyte phase, and for a purely planar system the steric factor is equal to 2. The overall rate constants k_{cd} and k_{d^*c} given by this treatment have therefore been divided by a factor of 2 to account approximately for the geometrical constraints imposed due to the adsorption of dye on the semiconductor surface (with slightly different values being appropriate for curvature on the particles and/or voids on the scale of molecular collision processes). The rate constant expression for the injection (k_{d^*s}) includes a bias dependence but does not, for simplicity, incorporate any effects associated with a shift in the conduction band edge as a function of potential. The rate constant expression for the leakage current, k_{oc}, is explicitly dependent on the electrode potential, as this reaction takes place at a conventional metal electrode/electrolyte interface that experiences a potential drop commensurate with changes in potential applied to the electrode.

D. Expressions for Charge-Carrier Generation. The flux of monochromatic radiation at a distance x into the film, measured from the conducting contact, is given by

$$\Psi(x) = \Psi_0\exp(-\ln 10\sum_i \epsilon_i\int_a^b C_i(u)\,\mathrm{d}u) \qquad (10.1)$$

where Ψ_0 is the incident photon flux (cm^{-2} s^{-1}), $C_i(x)$ is the concentration (cm^{-3}), and $\epsilon_i(\lambda)$ is the decadic extinction coefficient (cm^2) of the ith species. The thickness of the mesoporous semiconductor membrane is designated as δ, and the separation between the photoanode and metal film cathode, as measured from the position of the current-collecting contact to the semiconductor phase, is θ ($>\delta$). For illumination through the substrate/membrane interface ($x = 0$), $a = 0$ and $b = x$. For

illumination through the electrolyte/membrane interface ($x = \theta$), $a = \theta$ and $b = x$. For the special case where the cell is illuminated through $x = 0$ and the light-attenuating species are dispersed homogeneously,

$$\Psi(x) = \Psi_0 \exp(-\alpha x), \quad \text{where } \alpha = \ln 10(\sum_i \epsilon_i C_i) \quad (10.2)$$

In this case, the activation rate is given by

$$u^* = \xi\Psi(x)[d]\epsilon_d \ln 10 = \xi\alpha\beta\Psi_0 \exp(-\alpha x), \quad \text{where } \beta = \epsilon_d[d]/(\sum_i \epsilon_i C_i) \quad (11)$$

where $[d]$ is the effective dye concentration, in inverse cubic centimeters, in the membrane and the conversion factor ξ is defined in the following section.

E. Membrane Model. Some of the rate expressions require conversion from surface coverages, measured in molecules per square centimeter, to volumetric rate expressions based on concentrations measured in molecules per cubic centimeter. The exact value of this conversion factor depends on both the surface-to-volume ratio and the morphology of the particles in the membrane.

The electron or hole flux at the edge of the mesoporous semiconductor membrane ($x = \delta$) is limited to that which arises from interfacial electron transfer across that plane. The flux must be small due to the nanoporous nature of the semiconductor membrane because the projected surface area of any volume element is a very small fraction of its internal surface area. This same fraction will relate the flux of electrons through that volume element (U_i) to the interfacial electron-transfer flux (u_i) within it. The needed conversion factor, ξ, can therefore be broken down conceptually into two separate quantities: (1) $V/S_m = L$, which describes the ratio between the total volume of the membrane (including pore volume), V, and the total exposed surface area of the particles, S_m, and (2) a dimensionless quantity, γ, which describes the fraction of the area of a flux boundary plane at $x = \delta$ that supports interfacial electron-transfer reactions with the membrane.

For a periodic structure consisting of a three-dimensional array of identical, cubic particles joined at their corners, the unit cell contains two cubic particles, with the dimension of $3L/2$, occupies a cell volume of $27L^3$ ($=a^3$), and has an internal surface area of $27L^2$. Thus, the volume-to-area ratio is L, and the conversion factor ξ has a value of $3L/2$. For a cubic array of spheres, $\xi = \pi L/2$. Other packing structures, such as a body-centered-cubic or face-centered-cubic array of cubes, have conversion factors with numerical values very close to $3L/2$.

In the specific example of a cubic packing of particles, assuming that electron transfer proceeds isotropically through all six faces of the cube, then only one-sixth of this quantity will constitute a flux across the plane. Thus,

$$j_{n_s}(\delta) = \frac{U_{n_s}(\delta)L}{4} \quad \left(\text{or } j_{n_s}(\delta) = \frac{U_{n_s}(\delta)\xi}{6}\right) \quad (12)$$

where $j_{n_s}(\delta)$ is used to represent the electron flux at $x = \delta$. In cases where it is necessary to consider diffusion of dye holes, an analogous result is obtained. Slightly different numerical values of the denominator of eq 12 would be obtained for different membrane packing morphologies that possess anisotropic packing of particles normal to the flux boundary plane at $x = \delta$ relative to the particle packing parallel to the flux boundary plane.

For any membrane structure, in the limit of zero particle size, electron and hole fluxes vanish at the film edge. In this limit, the ionic flux is a continuous function over $0 \le x \le \theta$. In general, however, $j_{n_s}(\delta)$ and $j_{p_d}(\delta)$ are nonzero, and so the fluxes of n_c and p_c are discontinuous at $x = \delta$. When δ is approached from outside the membrane,

$$\lim_{x\to\delta^+} j_{p_c}(x) = -j \quad (13)$$

When δ is approached from within the membrane,

$$\lim_{x\to\delta^-} j_{p_c}(x) = -j + j_{n_s}(\delta) - j_{p_d}(\delta) \quad (14)$$

With the same argument as that used to evaluate the electron flux, the relationship between the effective dye concentration per unit volume in the membrane ($[d]$ in cm^{-3}) and the surface concentration of the dye per unit area ($[d]_{x=\delta}$ in cm^{-2}) in the case of a cubic membrane structure can be obtained using

$$[d]_{x=\delta} = [d]\left(\frac{L}{4}\right) \quad (15)$$

which is simply an expression of the fact that there are six faces on each cubic particle, with dyes equally adsorbed on each face.

F. Expressions for Charge-Carrier Transport. To a first approximation, drift can be neglected in nanoporous membranes impregnated with electrolyte. For charge carriers confined to an electrolyte phase, this approximation is excellent. However, Vanmaekelbergh et al. have shown that drift can contribute significantly to the transport of charge carriers in the semiconductor phase.[26] As shown in Appendix II, the effect of field-induced drift can be approximated by an enhancement of the apparent diffusion coefficient by a factor of $1 + f$ for systems where the applied potential (E) and the charge-carrier concentration (n_s) are related by

$$\frac{n_s}{n_{s,eq}} = \exp\left(-\frac{qE}{fk_BT}\right) \quad (16)$$

Incorporating this correction, Fick's laws can then be used to describe the transport of all charge carriers. At steady state,

$$\frac{\partial C_i}{\partial t} = D_i\left(\frac{\partial^2 C_i}{\partial x^2}\right) + \frac{u_i}{\xi} = 0 \quad (17)$$

where u_i ($cm^{-2}\ s^{-1}$) is the rate at which each species i is formed by chemical reaction, given by eqs 8.1−8.4, and ξ is the conversion factor obtained from the membrane model to obtain the corresponding homogeneous reaction rate.

For nondiffusing species, the steady-state condition requires simply that

$$\frac{\partial C_i}{\partial t} = \frac{u_i}{\xi} = 0 \quad (18)$$

Applying eqs 17 and 18 together with eqs 8.1−8.4, in which n_s, p_c, and n_c are subject to diffusion, yields

$$\xi\frac{d^2 n_s}{dx^2} = -\frac{1}{D_{n_s}(1+f)}\left(k_{d^*s}d^*(1-R_{d^*s}) - k_{sd}n_s p_d(1-R_{sd}) - k_{sc}n_s\sqrt{K_I\frac{p_c}{n_c}}(1-R_{sc})\right) \quad (19.1)$$

$$\xi \frac{d^2 p_c}{dx^2} = -\frac{1}{D_{p_c}}\left(-k_{d^*c} d^* \sqrt{K_I \frac{p_c}{n_c}} + k_{cd} n_c p_d (1 - R_{cd}) - k_{sc} n_s \sqrt{K_I \frac{p_c}{n_c}} (1 - R_{sc})\right) \quad (19.2)$$

$$\xi \frac{d^2 n_c}{dx^2} = -\frac{1}{D_{n_c}}\left(k_{d^*c} d^* \sqrt{K_I \frac{p_c}{n_c}} - k_{cd} n_c p_d (1 - R_{cd}) + k_{sc} n_s \sqrt{K_I \frac{p_c}{n_c}} (1 - R_{sc})\right) \quad (19.3)$$

$$u^* - d^*\left\{k_{d^*c}\sqrt{K_I \frac{p_c}{n_c}} + k_{d^*s}(1 - R_{d^*s}) + k_d\right\} = 0 \quad (20)$$

$$d^*\left\{k_{d^*s}(1 - R_{d^*s}) + k_{d^*c}\sqrt{K_I \frac{p_c}{n_c}}\right\} - p_d\{k_{sd} n_s (1 - R_{sd}) + k_{cd} n_c (1 - R_{cd})\} = 0 \quad (21)$$

It is convenient to recast eqs 19.1−19.3 in a form that does not depend on the concentration of the excited state of the dye. Quantum yields for quenching of the excited dye by the semiconductor and the contacting phase are defined, respectively, by

$$\phi_s = \frac{k_{d^*s}(1 - R_{d^*s})}{k_{d^*c}\sqrt{K_I \frac{p_c}{n_c}} + k_{d^*s}(1 - R_{d^*s}) + k_d} \quad (22.1)$$

$$\phi_c = \frac{k_{d^*c}\sqrt{K_I \frac{p_c}{n_c}}}{k_{d^*c}\sqrt{K_I \frac{p_c}{n_c}} + k_{d^*s}(1 - R_{d^*s}) + k_d} \quad (22.2)$$

Incorporating these substitutions, the diffusion equations become

$$\xi \frac{d^2 n_s}{dx^2} = -\frac{1}{D_{n_s}(1 + f)}\left(u^* \phi_s - k_{sd} n_s p_d (1 - R_{sd}) - k_{sc} n_s \sqrt{K_I \frac{p_c}{n_c}} (1 - R_{sc})\right) \quad (23.1)$$

$$\xi \frac{d^2 p_c}{dx^2} = -\frac{1}{D_{p_c}}\left(-u^* \phi_c + k_{cd} n_c p_d (1 - R_{cd}) - k_{sc} n_s \sqrt{K_I \frac{p_c}{n_c}} (1 - R_{sc})\right) \quad (23.2)$$

$$\xi \frac{d^2 n_c}{dx^2} = -\frac{1}{D_{n_c}}\left(u^* \phi_c - k_{cd} n_c p_d (1 - R_{cd}) + k_{sc} n_s \sqrt{K_I \frac{p_c}{n_c}} (1 - R_{sc})\right) \quad (23.3)$$

The steady-state concentration of oxidized dye ($[d^+]$) is the sum of its equilibrium value and the amount of holes generated due to the electron injection followed by the excitation of dyes. If dye holes are rapidly filled by regeneration and/or recombination, such that the steady-state concentration p_d is insignificant compared to the analytical concentration of the dye, then u^* is given by eq 11, with $[d] = [d]_0$. This assumption serves as a low-intensity limit and results in remarkable simplification, as shown in Appendix III. From eq 15, the rate of activation is given by

$$u^* = \xi \epsilon_d \ln 10([d]_0 - [d^+])\Psi_0 \exp\{-\ln 10 \int_0^x [\vartheta + \epsilon_{n_s} n_s + \epsilon_{n_c} n_c + \epsilon_{p_c} p_c + \epsilon_{p_d}[d^+] + \epsilon_d([d]_0 - [d^+])]\, du\} \quad (24)$$

where $[d]_0$ and $[d^+]$ are the effective concentrations (in cm^{-3}) of the dye initially present in the membrane and the dye holes, respectively. The quantity ϑ represents the absorption and scattering loss from components of the system, such as the semiconductor film itself, that are uniformly distributed and whose concentration does not change with time.

When the electrochemical potential of the solution is more positive than the formal potential of the d^+/d redox system, the initial concentration of d is not equal to $[d]_0$ but is instead dictated by the thermodynamically driven equilibration of the oxidized and reduced forms of the adsorbed dye with the redox species in the solution. In this situation, if additionally the oxidized dye is rapidly regenerated by redox species in solution, eq 24 still holds except that the initial dye concentration is smaller than the analytical concentration of dye, d_0. In another situation of interest, a significant fraction of the oxidized dye generated by injection may not be regenerated efficiently.[27] This situation is not incorporated into the simplified low-intensity limit expression of eq 24.

G. Dimensionless Expression of the Kinetics Equations. Because eqs 23−24 can be solved only with the aid of numerical integration, it is convenient to make use of dimensionless variables. The definitions of the dimensionless variables and some selected resulting equations that correspond to the dimensional forms of the equations shown above are listed in Table 2.

In dimensionless form, eqs 20 and 21 are conveniently combined to give eq D.5.3 (Table 2) and the diffusion equations (eqs 23.1−23.3) become

$$\frac{\xi}{\delta} \frac{d^2 \mathbf{N}_s}{dX^2} = -\frac{1}{\mathbf{D}_{n_s}}\left(\frac{u^* \phi_s}{\Psi_0} - \mathbf{k}_{sd} \mathbf{N}_s \mathbf{P}_d (1 - R_{sd}) - \mathbf{k}_{sc} \mathbf{N}_s \sqrt{\frac{K_I}{p_c^\circ n_c^\circ}} \sqrt{\frac{\mathbf{P}_c}{\mathbf{N}_c}} (1 - R_{sc})\right) \quad (25.1)$$

$$\frac{\xi}{\delta} \frac{d^2 \mathbf{P}_c}{dX^2} = -\frac{1}{\mathbf{D}_{p_c}}\left(-\frac{u^* \phi_c}{\Psi_0} + \mathbf{k}_{cd} \mathbf{N}_c \mathbf{P}_d (1 - R_{cd}) - \mathbf{k}_{sc} \mathbf{N}_s \sqrt{\frac{K_I}{n_c^\circ p_c^\circ}} \sqrt{\frac{\mathbf{P}_c}{\mathbf{N}_c}} (1 - R_{sc})\right) \quad (25.2)$$

$$\frac{\xi}{\delta} \frac{d^2 \mathbf{N}_c}{dX^2} = -\frac{1}{\mathbf{D}_{n_c}}\left(\frac{u^* \phi_c}{\Psi_0} - \mathbf{k}_{cd} \mathbf{N}_c \mathbf{P}_d (1 - R_{cd}) + \mathbf{k}_{sc} \mathbf{N}_s \sqrt{\frac{K_I}{n_c^\circ p_c^\circ}} \sqrt{\frac{\mathbf{P}_c}{\mathbf{N}_c}} (1 - R_{sc})\right) \quad (25.3)$$

Assuming that light at the wavelength of interest is attenuated

TABLE 2: Definition of Dimensionless Variables and Some Selected Equations with Dimensionless Variables

dimension and concentrations	diffusion coefficients
$x = X\delta$ (D.1.1)	$\mathbf{D}_{n_s} = \frac{D_{n_s} n_{s,\mathrm{eq}}(1+f)}{\Psi_0 \delta}$ (D.2.1)
$n_s = \mathbf{N}_s n_{s,\mathrm{eq}}$ (D.1.2)	$\mathbf{D}_{p_c} = \frac{D_{p_c} p_c^\circ}{\Psi_0 \delta}$ (D.2.2)
$p_c = \mathbf{P}_c p_c^\circ$ (D.1.3)	$\mathbf{D}_{n_c} = \frac{D_{n_c} n_c^\circ}{\Psi_0 \delta}$ (D.2.3)
$n_c = \mathbf{N}_c n_c^\circ$ (D.1.4)	
$p_d = \mathbf{P}_d d_0$ (D.1.5)	
$[d^+]_\delta = \mathbf{P}_d [d]_0$ (D.1.6)	
$p_c^\circ = 1.0 \times 10^{-3}$ mol cm^{-3}	$\Psi_0 = 9.87 \times 10^{16}$ cm^{-2} s^{-1}
$n_c^\circ = 1.0 \times 10^{-3}$ mol cm^{-3}	$\delta = 10^{-3}$ cm
$d_0 \approx 1.0 \times 10^{14}$ cm^{-2}	$D_{n_s} \approx 2.3 \times 10^{-5}$ cm^2 s^{-1}
$n_{s,\mathrm{eq}} \approx 1.0 \times 10^{17}$ cm^{-3}	$D_{p_c} = D_{n_c} \approx 1.0 \times 10^{-5}$ cm^2 s^{-1}

kinetics rate constants	extinction coefficients
$\mathbf{k}_{sc} = \frac{k_{sc} n_{s,\mathrm{eq}} p_c^\circ}{\Psi_0}$ (D.3.1)	$\mathbf{e}_{n_s} = \ln 10\ \delta n_{s,\mathrm{eq}} \epsilon_{n_s}$ (D.4.1)
$\mathbf{k}_{cd} = \frac{k_{cd} n_c^\circ d_0}{\Psi_0}$ (D.3.2)	$\mathbf{e}_{n_c} = \ln 10\ \delta n_c^\circ \epsilon_{n_c}$ (D.4.2)
$\mathbf{k}_{sd} = \frac{k_{sd} n_{s,\mathrm{eq}} d_0}{\Psi_0}$ (D.3.3)	$\mathbf{e}_{p_c} = \ln 10\ \delta p_c^\circ \epsilon_{p_c}$ (D.4.3)
$\mathbf{k}_{d^*s} = \frac{k_{d^*s}}{k_d}$ (D.3.4)	$\mathbf{e}_{p_d} = \ln 10\ \delta [d]_0 \epsilon_{p_d}$ (D.4.4)
$\mathbf{k}_{d^*c} = \frac{k_{d^*c} p_c^\circ}{k_d}$ (D.3.5)	$\mathbf{e}_d = \ln 10\ \delta [d]_0 \epsilon_d$ (D.4.5)
$\mathbf{k}_{oc} = \frac{f_A k_{oc}(E)(\mathbf{K}_\mathrm{I})^{1/2}}{\Psi_0}$ (D.3.6) (D.4.6)	$\mathbf{v} = \ln 10\ \delta \vartheta$ (D.4.6)
	$\epsilon_d \approx 2.0 \times 10^{-17}$ cm^2
	$\epsilon_{n_s} = \epsilon_{n_c} = \epsilon_{p_c} = 0$

quenching quantum yields (eqs 22.1 and 22.2)

$$\phi_s = \frac{\mathbf{k}_{d^*s}(1 - R_{d^*s})}{\mathbf{k}_{d^*c}\sqrt{\frac{K_\mathrm{I}}{n_c^\circ p_c^\circ}}\sqrt{\frac{\mathbf{P}_c}{\mathbf{N}_c}} + \mathbf{k}_{d^*s}(1 - R_{d^*s}) + 1} \quad \text{(D.5.1)}$$

$$\phi_c = \frac{\mathbf{k}_{d^*c}\sqrt{\frac{K_\mathrm{I}}{n_c^\circ p_c^\circ}}\sqrt{\frac{\mathbf{P}_c}{\mathbf{N}_c}}}{\mathbf{k}_{d^*c}\sqrt{\frac{K_\mathrm{I}}{n_c^\circ p_c^\circ}}\sqrt{\frac{\mathbf{P}_c}{\mathbf{N}_c}} + \mathbf{k}_{d^*s}(1 - R_{d^*s}) + 1} \quad \text{(D.5.2)}$$

eqs 20, 21, and 24

$$\frac{u^*}{\Psi_0} = \frac{\mathbf{p}_d[\mathbf{k}_{sd}\mathbf{N}_s(1 - R_{sd}) + \mathbf{k}_{cd}\mathbf{N}_c(1 - R_{cd})]}{\phi_s + \phi_c} \quad \text{(D.5.3)}$$

$$\frac{u^*\delta}{\Psi_0} = \frac{\xi}{\delta}\mathbf{e}_d(1 - \mathbf{p}_d)\exp\{-\int_0^x [\mathbf{v} + \mathbf{e}_{n_s}\mathbf{N}_s + \mathbf{e}_{n_c}\mathbf{N}_c + \mathbf{e}_{p_c}\mathbf{P}_c + \mathbf{e}_{p_d}\mathbf{P}_d + \mathbf{e}_d(1 - \mathbf{P}_d)]\,\mathrm{d}U\} \quad \text{(D.5.4)}$$

only by the dye and by species that are uniformly distributed within the membrane, eq D.5.4 (Table 2) becomes

$$\frac{u^*}{\Psi_0} = \frac{\xi}{\delta}\mathbf{e}_d(1 - \mathbf{p}_d)\exp\left\{-(\mathbf{v} + \mathbf{e}_d)X + \mathbf{e}_d\left(1 - \frac{\mathbf{e}_{p_d}}{\mathbf{e}_d}\right)\int_0^X \mathbf{P}_d\,\mathrm{d}U\right\} \quad (26)$$

Combining with eq D.5.3, we find

$$\frac{\mathbf{p}_d}{1 - \mathbf{p}_d} = \frac{\xi}{\delta}\frac{\mathbf{e}_d(\phi_s + \phi_c)\exp\left\{-(\mathbf{v} + \mathbf{e}_d)X + \mathbf{e}_d\left(1 - \frac{\mathbf{e}_{p_d}}{\mathbf{e}_d}\right)\int_0^X \mathbf{P}_d\,\mathrm{d}U\right\}}{[\mathbf{k}_{sd}\mathbf{N}_s(1 - R_{sd}) + \mathbf{k}_{cd}\mathbf{N}_c(1 - R_{cd})]} \quad (27)$$

Equation 27 is recognized as an additional differential equation to be solved along with eqs 25.1−25.3.

H. Boundary Conditions and the External Current Efficiency. Seven boundary conditions are required to solve the above system of equations, which consists of one first-order equation and three second-order differential equations. The first boundary condition is trivial. At $x = 0$,

$$\int_0^x p_d(u)\,\mathrm{d}u = 0 \quad (28)$$

By assumption, the interface between the semiconductor membrane and the conducting substrate is at equilibrium with respect to electron transfer. Hence,

$$\frac{n_s(0)}{n_{s,\mathrm{eq}}} = \exp\left[-\frac{qE(0)}{fk_\mathrm{B}T}\right] \quad (29)$$

Consider the charge-carrier fluxes on both sides of the semiconductor membrane. The leakage current density, $j_{n_c}(0)$, is given by

$$j_{n_c}(0) = -j_{p_c}(0) = -f_A(K_\mathrm{I})^{1/2}k_{oc}(E)\sqrt{\frac{p_c(0)}{n_c(0)}} \quad (30)$$

where $k_{oc}(E)$ is the potential dependent rate constant, eqs K.6.1 and K.6.2 in Table 1, between the electrons in the substrate (SnO_2) and the acceptor in the electrolyte (iodine atom in this case). The quantity f_A refers to the fraction of substrate area exposed to the contacting phase, and K_I is defined in eq 7.

Since the first derivative of any charge-carrier concentration is related by Fick's first law to its flux, from eq 30,

$$\left(\frac{\mathrm{d}n_c}{\mathrm{d}x}\right)_{x=0} = \frac{f_A k_{oc}(E)}{D_{n_c}}(K_\mathrm{I})^{1/2}\sqrt{\frac{p_c(0)}{n_c(0)}} \quad (31)$$

Similarly,

$$\left(\frac{\mathrm{d}p_c}{\mathrm{d}x}\right)_{x=0} = -\frac{f_A k_{oc}(E)}{D_{p_c}}(K_\mathrm{I})^{1/2}\sqrt{\frac{p_c(0)}{n_c(0)}} \quad (32)$$

It can be shown that the boundary condition at $x = \delta$ depends on the morphology of the semiconductor membrane (vide supra, section II.E). For films consisting of nanoparticles, $j_{n_s}(\delta) \approx 0$.

TABLE 3: Boundary Conditions with Dimensionless Variables

original eq	dimensionless eq
eq 28	$\int_0^X \mathbf{P}_d(U)\,\mathrm{d}U = 0 \quad \text{at} \quad X = 0$ (B.1)
eq 29	$\mathbf{N}_s(0) = \exp\left[-\frac{qE(0)}{fk_BT}\right]$ (B.2)
eq 31	$\left(\frac{\mathrm{d}\mathbf{N}_c}{\mathrm{d}X}\right)_{x=0} = \frac{\mathbf{k}_{oc}}{\mathbf{D}_{n_c}}\sqrt{\frac{p_c^\circ}{n_c^\circ}}\sqrt{\frac{\mathbf{P}_c(0)}{\mathbf{N}_c(0)}}$ ($\mathbf{k}_{oc}$ is defined by eq D.3.6 in Table 2) (B.3)
eq 32	$\left(\frac{\mathrm{d}\mathbf{P}_c}{\mathrm{d}X}\right)_{x=0} = \frac{\mathbf{k}_{oc}}{\mathbf{D}_{n_c}}\sqrt{\frac{p_c^\circ}{n_c^\circ}}\sqrt{\frac{\mathbf{P}_c(0)}{\mathbf{N}_c(0)}}$ ($\mathbf{k}_{oc}$ is defined by eq D.3.6 in Table 2) (B.4)
eq 33	$\left(\frac{\mathrm{d}\mathbf{N}_s}{\mathrm{d}X}\right)_{X=1} \approx 0$ (B.5)
eq 34	$\int_0^{\theta/\delta}\left[\frac{\mathbf{P}_c(X)}{\mu_O} + \frac{\mathbf{N}_c(X)}{\mu_R}\right]\mathrm{d}X = \frac{\theta}{\delta}\left(\frac{p_{c,0}}{\mu_O p_c^\circ} + \frac{n_{c,0}}{\mu_R n_c^\circ}\right)$ (B.6)
eq 36	$\int_0^{\theta/\delta}\left[\{\mathbf{N}_s(X) - 1\}\frac{n_{s,eq}}{n_c^\circ - p_c^\circ} - \mathbf{P}_d(X)\frac{d_0^m}{n_c^\circ - p_c^\circ} + \mathbf{N}_c(X)\frac{n_c^\circ}{n_c^\circ - p_c^\circ} - \mathbf{P}_c(X)\frac{p_c^\circ}{n_c^\circ - p_c^\circ}\right]\mathrm{d}X = \frac{\theta}{\delta}$
eqs 37 and 38	$\int_0^{\theta/\delta}\mathbf{P}_c(X)\,\mathrm{d}X = \frac{\theta p_{c,0}}{p_c^\circ \delta} = \frac{\theta}{\delta}\frac{p_{c,0}}{p_c^\circ}$ (B.8) $\qquad$ $\int_0^{\theta/\delta}\mathbf{N}_c(X)\,\mathrm{d}X = \frac{\theta n_{c,0}}{n_c^\circ \delta} = \frac{\theta}{\delta}\frac{n_{c,0}}{n_c^\circ}$ (B.9)

Thus,

$$\left(\frac{\mathrm{d}n_s}{\mathrm{d}x}\right)_{x=\delta} \approx 0 \tag{33}$$

The last two boundary conditions can be obtained from mass balance and balance of redox equivalents. If the analytical concentrations of electrons and holes initially present in the contacting phase are denoted as $n_{c,0}$ and $p_{c,0}$, respectively, then for a generalized redox reaction,

$$\mu_O \mathrm{O} + \nu_{sc}\mathrm{e}^- \rightleftarrows \mu_R \mathrm{R} \tag{34}$$

conservation of the atomic constituents of the redox couple gives

$$\int_0^\theta \left[\frac{p_c(x)}{\mu_O} + \frac{n_c(x)}{\mu_R}\right]\mathrm{d}x = \theta\left(\frac{p_{c,0}}{\mu_O} + \frac{n_{c,0}}{\mu_R}\right) \tag{35}$$

and conservation of redox equivalents gives

$$\int_0^\theta [n_s(x) - n_{s,eq} - [d^+] + n_c(x) - p_c(x)]\,\mathrm{d}x = \theta(n_c^\circ - p_c^\circ) \tag{36}$$

If the concentration of the redox species in the contacting phase is much larger than that of electrons in the semiconductor or holes in the dye, then the last two boundary conditions can be replaced by simpler, approximate forms,

$$\int_0^\theta p_c(x)\,\mathrm{d}x = \theta p_{c,0} \tag{37}$$

$$\int_0^\theta n_c(x)\,\mathrm{d}x = \theta n_{c,0} \tag{38}$$

The dimensionless forms of the above boundary conditions are listed in Table 3.

Finally, outside of the membrane ($\delta \le x \le \theta$) neither electrons nor holes are created. By Fick's second law, the concentration profiles of p_c and n_c must be linear. This allows application of the dimensionless form of the boundary conditions in eqs 37 and 38 (eqs B.8 and B.9 in Table 3) while carrying the integration no farther than $X = 1$. Hence,

$$\int_0^1 \mathbf{P}_c(X)\,\mathrm{d}X = \frac{p_{c,0}}{p_c^\circ}\left(\frac{\theta}{\delta}\right) - \mathbf{P}_c(1)\left(\frac{\theta}{\delta} - 1\right) - \frac{\mathbf{P}_c'(1)}{2}\left(\frac{D_{out}}{D_{in}}\right)\left(\frac{\theta}{\delta} - 1\right)^2 \tag{39}$$

$$\int_0^1 \mathbf{N}_c(X)\,\mathrm{d}X = \frac{n_{c,0}}{n_c^\circ}\left(\frac{\theta}{\delta}\right) - \mathbf{N}_c(1)\left(\frac{\theta}{\delta} - 1\right) - \frac{\mathbf{N}_c'(1)}{2}\left(\frac{D_{out}}{D_{in}}\right)\left(\frac{\theta}{\delta} - 1\right)^2 \tag{40}$$

The diffusion coefficient of a species confined to the pores of the semiconductor membrane will be smaller than the diffusion coefficient of the same species outside of the membrane. The ratio of diffusion coefficients, which appears in the expressions above, is denoted D_{out}/D_{in} and is assumed to be independent of the diffusing species.

The external current efficiency is obtained from the computed charge-carrier fluxes. The external current density (j) is the difference between the contribution from the semiconductor and the leakage current from the contacting phase,

$$j = j_{n_s}(0) - j_{n_c}(0) \tag{41}$$

$$j = -D_{n_s}(1 + f)\left(\frac{\mathrm{d}n_s}{\mathrm{d}x}\right)_{x=0} + D_{n_c}\left(\frac{\mathrm{d}n_c}{\mathrm{d}x}\right)_{x=0} \tag{42}$$

$$\frac{j}{\Psi_0} = -\mathbf{D}_{n_s}\left(\frac{\mathrm{d}\mathbf{N}_s}{\mathrm{d}X}\right)_{X=0} + \mathbf{D}_{n_c}\left(\frac{\mathrm{d}\mathbf{N}_c}{\mathrm{d}X}\right)_{X=0} \tag{43}$$

Alternatively, in the contacting phase, $j_{n_c}(\delta) = -j_{p_c}(\delta) = j$.

Thus,

$$\frac{j}{\Psi_0} = -\mathbf{D}_{n_c}\left(\frac{\mathrm{d}\mathbf{N}_c}{\mathrm{d}X}\right)_{X=1} = \mathbf{D}_{p_c}\left(\frac{\mathrm{d}\mathbf{P}_c}{\mathrm{d}X}\right)_{X=1} \quad (44)$$

III. Discussion

A. Features of the Model. The model described above incorporates expressions for the simultaneous transport of three different charge carriers: reduced species and oxidized species in the solution, and electrons in the semiconductor membrane phase. The model also explicitly incorporates the membrane morphology in determining the electron-transfer fluxes that produce the charge-carrier motion in the semiconductor and liquid phases. The model additionally explicitly relates, within a single formalism, the rate constants for charge transfer in the membrane electrode system to conventional intramolecular and intermolecular electron-transfer rate constant expressions and to interfacial electron-transfer processes at planar metallic or semiconducting electrodes. Finally, the model is applicable to systems in which the rate processes of interest are reversible or near-reversible thermodynamically, allowing its applicability to a wide range of possible combinations of semiconductor, sensitizer, and ground and excited state energies of the dye. The system of differential equations, subject to the specified boundary conditions, represents a closed-form mathematical description of the charge-carrier flow in the electrochemical cell. This set of equations is readily solvable using numerical methods, thereby producing an analytical description of the current−voltage behavior of this photoelectrochemical cell under various conditions of experimental interest.

B. Treatment of the Interfacial Potential Drop across the Various Interfaces in the Nanostructured Semiconductor-Based Photoelectrochemical Cell. Prior to recent interest in nanostructured systems, semiconductor photoelectrochemistry dealt primarily with smooth semiconductor/solution interfaces. In these systems, depletion of charge carriers from dopants in the semiconductor lattice is the means by which equilibrium is achieved.[28−30] Because the differential capacitance of the resulting space-charge layer is typically small compared to that of the Helmholtz layer, any difference in electric potential between the semiconductor and the solution is dropped within the space-charge region. Extraction of electrons in the semiconductor by acceptor species in solution is given by

$$\frac{\mathrm{d}n}{\mathrm{d}t} = -kC_A n_i \quad (45)$$

where C_A is the concentration of the acceptor, n_i is the concentration of electrons at the interface, and k is a rate constant.

The situation is different for semiconductor nanoparticles, which because of their small size cannot develop an appreciable space charge.[31] In this case, virtually all of the potential must drop across the Helmholtz layer. The model developed herein neglects the dependence on the potential applied to the electrode of the interfacial rate constants from the semiconductor to the electrolyte phase. This approach is justified physically by the notion that all of the semiconductor particles, except for those in intimate contact with the substrate, are effectively screened from changes in the applied potential by virtue of penetration of the electrolyte into the membrane phase. This is consistent with the results of Zaban et al.[32] The portion of the TiO_2 layer that significantly experiences the potential applied to the conducting substrate can in principle extend deeper into the membrane as the applied bias is increased, and hence an empirical quality factor, f, is included to account for these various nonidealities. Therefore, eq 16, based on the Boltzmann equation, should be applied only to parts of the membrane that are at equilibrium with the conducting substrate, and it is reasonable to define a boundary condition at the current-collecting contact ($x = 0$) based on this relationship.

A related issue involves the use of Butler−Volmer versus Marcus type expressions to describe the interfacial rate processes at mesoporous electrode/electrolyte interfaces. The ruthenium complexes used to sensitize TiO_2 are typically 14 Å in diameter, and the dye molecules lie primarily outside of the nanocrystalline semiconductor particle's Helmholtz layer, which can be 3 or 4 Å in depth. When the transition state for electron-transfer experiences part (or all) of the potential drop across the interface, Butler−Volmer kinetics could be useful, and this formalism has been applied to describe the interfacial charge-transfer kinetics, particularly for the reduction of triiodide (k_{sc}) at TiO_2-based photoelectrodes.[11,20,33] A more general approach, adopted herein, involves the use of Marcus theory to describe the interfacial charge-transfer rate constants, along with the use of an appropriate free energy term for each elementary rate process, for all of the interfaces in the cell. The Marcus inverted effect is clearly incorporated in the equations for the recombination process (eq K.2, Table 1), which exhibits a Gaussian dependence on the driving force $-\Delta G^{\circ\prime}$, so that when $-\Delta G^{\circ\prime} > \lambda$, the rate constant should decrease with increasing driving force. The time-dependent spectroscopic data on the recombination processes for a series of metal polypyridyl complexes adsorbed on TiO_2 photoelectrodes are consistent with inverted region behavior.[34]

The rate constants are clearly a function of the interfacial energetics of the various components of the system. Injection of electrons into the particles of the semiconductor membrane ought to produce a shift in the band-edge position of such particles, thereby affecting the rate constants for the various charge-transfer processes in the system. However, when the effects of additional injected negative charge are screened, for example by intercalation of cations into the TiO_2 membrane, such changes in interfacial energetics are minimized. The most general treatment of the system would specifically relate the driving force for each rate process to the electron concentration on each particle. In the present treatment, we have assumed that such changes are largely screened by the electrolyte of interest and have therefore not incorporated such time-dependent energetic changes into the rate constant expressions of the system. Various other nonuniformities on the microscale are incorporated implicitly into the model by allowing for the possibility of a nonideal diode quality factor, f, as in eq 2.

C. Treatment of the Rate Constant for Electron Injection. The rate constant for charge injection from the electronically excited state of an adsorbed dye molecule into the conduction band of the semiconductor (k_{d^*s}) is expressed in the model described above through eqs K.1.1 and K.1.2 (Table 1). This approach is an extension of the Marcus theory of nonadiabatic electron transfer by incorporating a continuum of electronic states in the semiconductor conduction band as the electron acceptor species. The complement of the Fermi occupancy factor, $1 - F(\mathbf{E},E)$, has been used to account for the fact that electron injection occurs only into the empty states of the conduction band.[35] Here, $|H_{d^*s}|^2$ is the electronic coupling between the dye excited state and each conduction band state of the electrode (but assumed to be state-independent), $\Delta G^{\circ\prime}_{d^*s}(\mathbf{E})$ is the electrochemical potential difference between the excited state of the adsorbed dye, $qE^{\circ\prime}(d^{*+}/d^*)$, and the

conduction band state with energy **E** ($\mathbf{E} < \mathbf{E}_{cb}$), and λ_{d^*s} is the reorganization energy associated with electron injection. The quantity $\rho_{TiO_2,eff}$ is the effective density of states (DOS) of the conduction band of TiO_2.

The energy dependence of $\rho_{TiO_2,eff}$ should rigorously have been included in the argument of the integration of eq K1.2 because, unlike the case at a metal electrode, the DOS at a given energy level (**E**) is proportional to the square root of the difference in energy between the conduction band edge and the injecting state of the excited dye molecule. However, taking $\rho_{TiO_2,eff}$ as constant with energy in the conduction band is a very reasonable approximation in many systems because electron injection is an isoenergetic process and because generally the DOS is high enough at the energy of the excited state of the dye, $qE^{\circ\prime}(d^{*+}/d^*)$ so that injection proceeds under optimally exoergic conditions for the Franck−Condon portion of the rate constant of eq K.1.1. For systems in which the injection process only proceeds from states very near the bottom of the conduction band, a correction would be applied to the injection integral to account for the limited number of acceptor states in a given energy range and to account for the energy dependence of the state density in the TiO_2. Similarly, for systems in which the injection process is adiabatic, a correction can be applied so that the rate constant parameter produced by the model is not the value obtained from eqs K.1.1. and K.1.2 but instead properly quantifies the injection rate constant to include injection processes that are not in equilibrium with the dynamics of the solvent. These corrections can readily be incorporated as a change in the parametrized value of k_{d^*s} that is input into the kinetics model simulation,[36] without affecting the description or computation of the other transport and recombination processes that have been represented by the set of equations described above.

D. Behavior of Systems near Equilibrium. All of the near-equilibrium situations, in which reverse electron-transfer effects need to be considered for each rate process, have been simply but rigorously parametrized by introducing an *R* factor, R_{ij}, (Appendix I) into the relevant equations. Generally, the exact value of each *R* factor can be calculated from the electrochemical potentials of the components of cell. In this fashion, the model can be applied even when some of the processes in the cell are kinetically reversible, such as when a relatively small driving force exists to regenerate the reduced form of the dye by electron transfer from the reduced form of the redox species in the solution.

A restriction on the rigorous use of the model for treating kinetically reversible processes arises when dealing with the electron injection process. The "exact" principle of detailed balance was not applied to the microscopic reverse of the processes that describe charge injection from the excited state of the dye into the continuum of electronic states in the semiconductor conduction band. Transfer of hot electrons from the conduction band to the excited state of the dye was neglected because in general thermalization of injected electrons is quite rapid. Instead, the reverse electron transfer to the excited and oxidized dye (d^{*+}) was assumed to occur only from electrons having an energy at the bottom of the conduction band. In a more general approach, the principles of detailed balance and microscopic reversibility would be applied explicitly to all of the energy states in the semiconductor, including those representing the nonthermalized electron distribution in the conduction band of the TiO_2. However, more complicated rate expressions are produced as a result of introducing this added degree of rigor. The final parametrization values for modeling the steady state $J-E$ behavior of interest can be represented self-consistently within the current framework through a modification of the reverse rate constant value to account for the presence of such reverse electron injection processes, as appropriate. In this case, modification of the nondimensional parameter, *R*, to capture the overall reversibility of the electron injection forward and reverse reaction rate processes for the system of interest would generally suffice to account for this situation at steady state.

E. Kinetics of the Iodide/Triiodide Redox Couple. The description of the kinetics involving the redox system in the electrolyte is an extension of the dissociative chemisorption of iodine (I_2) at platinum (Pt) electrodes in aqueous solution.[22] However, this portion of the model can be modified without loss of generality to describe another electron-transfer process as appropriate. Two main issues need to be considered when different electron-transfer schemes are applied. The first is the identification of the actual acceptor and establishment of the relation between the concentration of the acceptor and that of the charge carriers (e.g. eq 7). The second issue concerns the free energy change ($\Delta G_{ij}^{\circ\prime}$) for the electron transfer from one phase (*i*) to another (*j*). Knowledge of the energy (or potential) of the actual acceptor state is crucial because this energy is not necessarily the same as the equilibrium potential of the solution, $E^{\circ\prime}(A/A^-)$. For example, $E^{\circ\prime}(A/A^-)$ is $E^{\circ\prime}(I_3^-/I^-)$ for the model used in this study, while the actual one-electron acceptor level is assumed to have a formal potential of $E^{\circ\prime}(I/I^-)$. Without taking this information into consideration, it is very difficult to have all the fitting parameters (e.g. $\Delta G_{ij}^{\circ\prime}$, λ_{ij}, and R_{ij}), shown in Table 1, described self-consistently. Expressions for $\Delta G_{ij}^{\circ\prime}$ for the present model are shown in Table 1. Regardless of the microscopic rate description used to describe the process, the final output is a parametrized value of the rate constants, k_{sc}, k_{cd}, k_{d^*c}, and k_{oc}, so adjustment of these values as a model input can be used to account for different kinetics schemes as appropriate.

Another reaction scheme for the I_3^-/I^- system, a two-step reduction mechanism, has been suggested recently on the basis of the observation of $I_2^{\bullet-}$ as an intermediate in the reduction of the redox species in the electrolyte.[19,37] In this model, the reduction reaction with I_3^- is second order in electron concentration,[19,38−40] with the corresponding kinetics pathway characterized by the formation of $I_2^{\bullet-}$ by the direct reduction of I_2, which is formed by the fast chemical equilibrium between I_3^- and I^-. The subsequent path suggested is either (A) the disproportionation of this intermediate ($I_2^{\bullet-}$) to iodide and triiodide or (B) the further reduction of $I_2^{\bullet-}$ to iodide by a direct electron transfer. In addition to the second-order dependence in the electron concentration of the reaction rate between electrons and I_3^-,[19,41,42] the former path, A, shows second-order kinetics with respect to the iodide/triiodide ratio[20,33] while the reaction is first order for the latter path, B. However, the reaction order with respect to the triiodide/iodide concentration ratio ($[I_3^-]/[I^-]$) is not well-established, and additionally it is not clear whether this two-step reduction process is the only mechanism consistent with the data.[42] A different mechanism, with a different reaction order, could be straightforwardly incorporated into the overall theoretical framework presented in this work, provided that the overall reaction scheme is composed of a series of reactions with a rate-determining single-electron-transfer step.

F. Implications of a Distribution of Diffusion Coefficients, Injection Rate Constants, and Recombination Rate Constants. Experimental measurements have in many cases been interpreted as providing evidence for a distribution of rate

constants for a variety of processes at nanocrystalline TiO_2 photoelectrodes. Specifically, a distribution of charge-transfer diffusion coefficients has been observed in transient photocurrent measurements, and stretched exponentials are often used to fit the dynamics of electron injection from the excited state of the dye into the semiconductor membrane phase. Similarly, transient measurements of the recombination rate between the injected electrons and the oxidized form of the dye are best fitted to a sum of two second-order rate constants. Finally, a distribution of trapping and detrapping events has been invoked to describe the strong dependence of the ambipolar diffusion coefficient upon the photoexcitation density.[43] Collectively, these effects presumably arise from the heterogeneity of adsorption sites, particle sizes, and other factors present in the nanocrystalline TiO_2 membrane electrode.

The dispersion in such rate processes cannot rigorously be described within the framework of the single set of differential equations presented herein. A one-dimensional treatment of diffusion, for carriers in the membrane and in the electrolyte, as used in the present model, is appropriate for a description of steady-state transport on the macroscale in isotropic structures such as randomly oriented networks of semiconductor particles in contact with a liquid electrolyte. A full treatment of a system having an energy-, space-, and time-dependent set of rate constants requires an extensive digital simulation model of the system of interest. In contrast, a single, effective value of the rate constant for each process has been used in the present modeling effort. To the extent that one rate constant dominates the behavior of each rate process at steady state, use of the appropriate rate constants in the model expression ought to provide a good basis for using the model to predict the resultant $J-E$ behavior of the system. The validity of this aspect of the modeling is evident in more detail when simulated $J-E$ curves are evaluated for specific cases of interest, as discussed in the following manuscript in this issue.

For generality, the effects of surface state recombination are implicitly incorporated into the present model in two forms. First, the recombination rate constant, k_{sd}, and the direct-reduction rate constant, k_{sc}, can be treated as input parameters that are decoupled from the other kinetics parameters, and thus, they can be varied independently to account for increased recombination that occurs via surface trapping pathways relative to recombination that occurs from charge carriers in the bands of the semiconducting solid. Second, the reaction order for such recombination, along with other nonidealities that might be displayed by the system, is incorporated phenomologically through a nonunity diode quality factor, f, in eq 2. Some TiO_2-based systems of current interest, with some TiO_2 preparations, have been reported to have a large density of surface traps. Other systems with either TiO_2 or other semiconductors and/or dyes may not be dominated by trap levels, and still others may exhibit yet different behavior such as nonuniform electric fields in the membrane, that will possibly lead to similar overall rate constants for recombination as those simulated herein, for a wide range of different experimental cases. The present model is not a microscopic model developed for one system on the basis of a specific behavior of that individual cell but instead, through the procedures described above, is generalizable and allows incorporation of the rate constant parameters that can be determined from dynamics experiments to ascertain whether the steady-state $J-E$ behavior is consistent with the values determined from the dynamics experiments and how the $J-E$ behavior will change as certain physical properties of the system are varied.

IV. Summary

An analytical model describing the operation of dye-sensitized nanocrystalline semiconductor photoelectrodes has been developed. The rate constants of the physical and chemical factors that determine carrier transport, recombination, and generation are parametrized in this model and can be used as independent variables to describe the overall $J-E$ characteristics of a dye-sensitized nanocrystalline semiconductor-based photoelectrode. The model includes the near-equilibrium situation, so that the reverse electron-transfer rates can be evaluated self-consistently. The semiclassical Marcus treatment has been incorporated to obtain rate constant expressions for the interfacial electron-transfer steps in the cell. Additionally, the model relates explicitly, within a single formalism, the rate constants for charge transfer of the membrane electrode system to conventional intramolecular and intermolecular electron-transfer rate constant expressions and to interfacial electron-transfer processes at planar metal or semiconductor electrodes. The system of differential equations, subject to the specified boundary conditions, represents a closed-form mathematical description of the charge-carrier flow in the system. This set of equations is readily solvable using numerical methods, thereby providing an analytical description of the current−voltage behavior of this type of photoelectrochemical cell.

Acknowledgment. The authors gratefully acknowledge the Department of Energy, Office of Basic Energy Sciences, for support of this work.

Appendix I

For given chemical or electrochemical reactions that include a charge-transfer process, one can relate the forward and reverse rate constants, with an appropriate equilibrium constant (K), by applying the principle of microscopic reversibility under equilibrium conditions.[44] For example, consider the reaction

$$\mathrm{A} + \mathrm{B} \underset{k_r}{\overset{k_f}{\rightleftharpoons}} \mathrm{C} + \mathrm{D} \qquad \text{(A.1.1)}$$

where k_f and k_r are the rate constants for the forward and reverse reactions, respectively. The overall rate of this reaction is expressed by the net flux calculated by subtracting the reverse reaction rate from the forward reaction rate.

$$\text{rate} = k_f[\mathrm{A}][\mathrm{B}] - k_r[\mathrm{C}][\mathrm{D}] \qquad \text{(A.1.2)}$$

At equilibrium, no net reaction occurs because the reverse reaction occurs at the same rate as that of the forward reaction. Thus, by setting the net rate to zero in eq A.1.2, the relationship between forward and reverse rate constants can be obtained in conjunction with an appropriate equilibrium constant, K.

$$K = \frac{k_f}{k_r} = \frac{[\mathrm{C}]_{eq}[\mathrm{D}]_{eq}}{[\mathrm{A}]_{eq}[\mathrm{B}]_{eq}} \qquad \text{(A.1.3)}$$

The equilibrium constant can be obtained from thermodynamics if the free energy (or electrochemical potential) change for the reaction is known:

$$\Delta G^{\circ\prime} = -RT \ln K \qquad \text{(A.1.4)}$$

According to the principle of microscopic reversibility, any elementary chemical transformation has the same values of its forward and reverse rate constants at equilibrium even if the system is away from equilibrium. Thus, the rate expression

under nonequilibrium conditions can be written as

$$\text{rate} = k_f[A][B]\left(1 - \frac{k_r[C][D]}{k_f[A][B]}\right) = k_f[A][B]\left(1 - \frac{1[C][D]}{K[A][B]}\right) \quad (A.1.5)$$

Here, the last term in the parentheses is simply a reaction quotient (Q) divided by the equilibrium constant (K) of this system and can be defined as R ($=Q/K$), to simplify the overall rate equation to

$$\text{rate} = k_f[a][b](1 - R) \quad (A.1.6)$$

The factor R is essentially a dimensionless quantity that serves as a measure of the reversibility of the process of interest at any instant in time. In other words, the degree of reversibility can be parametrized by R, with the reaction being totally irreversible if R is zero and in complete equilibrium when $R = 1.0$.

Appendix II

Transport of electrons through the mesoporous membrane is described by the usual combination of Fick and Nernst−Plank laws,

$$\frac{\partial n_s}{\partial t} = D_{n_s}\frac{\partial}{\partial x}\left[\frac{\partial n_s}{\partial x} - \frac{n_s F}{RT}\frac{\partial E}{\partial x}\right] + u_{n_s} \quad (A.2.1)$$

If the potential in the contacting phase is invariant, then the potential is related to the electron concentration by eq 16, or equivalently,

$$E = -\frac{fk_BT}{q}\ln\left(\frac{n_s}{n_{s,eq}}\right) \quad (A.2.2)$$

The derivative is

$$\frac{\partial E}{\partial x} = -\frac{fk_BT}{qn_s}\frac{\partial n_s}{\partial x} \quad (A.2.3)$$

and therefore,

$$\frac{\partial n_s}{\partial t} = D_{n_s}(1 + f)\frac{\partial^2 n_s}{\partial x^2} + u_{n_s} \quad (A.2.4)$$

Appendix III

In the low-intensity limit, u^* is given by eq 11, with $[d] = [d]_0$. Using the substitutions in eqs 23.1−23.3, for the diffusing species,

$$\xi\frac{d^2 n_s}{dx^2} = -\frac{1}{D_{n_s}(1+f)}\left(\xi\alpha\beta\phi_s\Psi_0\exp(-\alpha x) - k_{sd}n_s p_d(1 - R_{sd}) - k_{sc}n_s\sqrt{K_I\frac{p_c}{n_c}}(1 - R_{sc})\right) \quad (A.3.1)$$

$$\xi\frac{d^2 p_c}{dx^2} = -\frac{1}{D_{p_c}}\left(-\xi\alpha\beta\phi_c\Psi_0\exp(-\alpha x) + k_{cd}n_c p_d(1 - R_{cd}) - k_{sc}n_s\sqrt{K_I\frac{p_c}{n_c}}(1 - R_{sc})\right) \quad (A.3.2)$$

$$\xi\frac{d^2 n_c}{dx^2} = -\frac{1}{D_{n_c}}\left(\xi\alpha\beta\phi_c\Psi_0\exp(-\alpha x) - k_{cd}n_c p_d(1 - R_{cd}) + k_{sc}n_s\sqrt{K_I\frac{p_c}{n_c}}(1 - R_{sc})\right) \quad (A.3.3)$$

and for dye holes,

$$p_d = \xi\frac{\alpha\beta(\phi_s + \phi_c)\Psi_0\exp(-\alpha x)}{k_{sd}n_s(1 - R_{sd}) + k_{cd}n_c(1 - R_{cd})} \quad (A.3.4)$$

The dimensionless diffusion coefficients and rate functions now incorporate β for convenience.

$$\mathbf{D}_{n_s} = \frac{D_{n_s}n_{s,eq}(1+f)}{\beta\Psi_0\delta} \quad (A.3.5)$$

$$\mathbf{D}_{p_c} = \frac{D_{p_c}p_c^\circ}{\beta\Psi_0\delta} \quad (A.3.6)$$

$$\mathbf{D}_{n_c} = \frac{D_{n_c}n_c^\circ}{\beta\Psi_0\delta} \quad (A.3.7)$$

$$\mathbf{k}_{sc} = \frac{k_{sc}n_{s,eq}p_c^\circ}{\beta\Psi_0} \quad (A.3.8)$$

$$\mathbf{k}_{cd} = \frac{k_{cd}n_c^\circ d_0}{\beta\Psi_0} \quad (A.3.9)$$

$$\mathbf{k}_{sd} = \frac{k_{sd}n_{s,eq}d_0}{\beta\Psi_0} \quad (A.3.10)$$

For convenience,

$$\mathbf{A} = \alpha\delta \quad (A.3.11)$$

These substitutions afford the following set of differential equations:

$$\frac{\xi}{\delta}\frac{d^2\mathbf{N}_s}{dX^2} = -\frac{1}{\mathbf{D}_{n_s}}\left(\frac{\xi}{\delta}A\phi_s\exp(-AX) - \mathbf{k}_{sd}\mathbf{N}_s\mathbf{P}_d(1 - R_{sd}) - \mathbf{k}_{sc}\mathbf{N}_s\sqrt{\frac{K_I}{p_c^\circ n_c^\circ}}\sqrt{\frac{\mathbf{P}_c}{\mathbf{N}_c}}(1 - R_{sc})\right) \quad (A.3.12)$$

$$\frac{\xi}{\delta}\frac{d^2\mathbf{P}_c}{dX^2} = -\frac{1}{\mathbf{D}_{p_c}}\left(-\frac{\xi}{\delta}A\phi_c\exp(-AX) + \mathbf{k}_{cd}\mathbf{N}_c\mathbf{P}_d(1 - R_{cd}) - \mathbf{k}_{sc}\mathbf{N}_s\sqrt{\frac{K_I}{p_c^\circ n_c^\circ}}\sqrt{\frac{\mathbf{P}_c}{\mathbf{N}_c}}(1 - R_{sc})\right) \quad (A.3.13)$$

$$\frac{\xi}{\delta}\frac{d^2\mathbf{N}_c}{dX^2} = -\frac{1}{\mathbf{D}_{n_c}}\left(\frac{\xi}{\delta}A\phi_c\exp(-AX) - \mathbf{k}_{cd}\mathbf{N}_c\mathbf{P}_d(1 - R_{cd}) + \mathbf{k}_{sc}\mathbf{N}_s\sqrt{\frac{K_I}{p_c^\circ n_c^\circ}}\sqrt{\frac{\mathbf{P}_c}{\mathbf{N}_c}}(1 - R_{sc})\right) \quad (A.3.14)$$

From eq A.3.4 we obtain

$$\mathbf{P}_d = \frac{\xi}{\delta}\frac{A(\phi_s + \phi_c)\exp(-AX)}{\mathbf{k}_{sd}\mathbf{N}_s(1 - R_{sd}) + \mathbf{k}_{cd}\mathbf{N}_c(1 - R_{cd})} \quad \text{(A.3.15)}$$

This system is solved according to the same boundary values outlined for the general case.

References and Notes

(1) Hagfeldt, A.; Grätzel, M. *Acc. Chem. Res.* **2000**, *33*, 269−277.
(2) Moser, J. E.; Bonnote, P.; Grätzel, M. *Coord. Chem. Rev.* **1998**, *171*, 245−250.
(3) Kalyanasundaram, K.; Grätzel, M. *Coord. Chem. Rev.* **1998**, *177*, 347−414.
(4) Hagfeldt, A.; Grätzel, M. *Chem. Rev.* **1995**, *95*, 49−68.
(5) Grätzel, M.; Kalyanasundaram, K. *Curr. Sci.* **1994**, *66*, 706−714.
(6) Grätzel, M. *Coord. Chem. Rev.* **1991**, *111*, 167−174.
(7) Södergren, S.; Hagfeldt, A.; Olsson, J.; Lindquist, S. E. *J. Phys. Chem.* **1994**, *98*, 5552−5556.
(8) Cao, F.; Oskam, G.; Meyer, G. J.; Searson, P. C. *J. Phys. Chem.* **1996**, *100*, 17021−17027.
(9) Dloczik, L.; Ileperuma, O.; Lauermann, I.; Peter, L. M.; Ponomarev, E. A.; Redmond, G.; Shaw, N. J.; Uhlendorf, I. *J. Phys. Chem. B* **1997**, *101*, 10281−10289.
(10) Ferber, J.; Stangl, R.; Luther, J. *Sol. Energy Mater.* **1998**, *53*, 29−54.
(11) Ferber, J.; Luther, J. *J. Phys. Chem. B* **2001**, *105*, 4895−4903.
(12) Stangl, R.; Ferber, J.; Luther, J. *Sol. Energy Mater.* **1998**, *54*, 255−264.
(13) Schwarzburg, K.; Willig, F. *J. Phys. Chem. B* **1999**, *103*, 5743−5746.
(14) Some models use exactly the same formula except that the recombination is second order with respect to the electrons in the semiconductor. For example, see refs 19 and 20.
(15) Pichot, F.; Gregg, B. A. *J. Phys. Chem. B* **2000**, *104*, 6−10.
(16) van de Lagemaat, J.; Park, N. G.; Frank, A. J. *J. Phys. Chem. B* **2000**, *104*, 2044−2052.
(17) Cahen, D.; Hodes, G.; Gratzel, M.; Guillemoles, J. F.; Riess, I. *J. Phys. Chem. B* **2000**, *104*, 2053−2059.
(18) Peter, L. M.; Ponomarev, E. A.; Franco, G.; Shaw, N. J. *Electrochim. Acta* **1999**, *45*, 549−560.
(19) Fisher, A. C.; Peter, L. M.; Ponomarev, E. A.; Walker, A. B.; Wijayantha, K. G. U. *J. Phys. Chem. B* **2000**, *104*, 949−958.
(20) Huang, S. Y.; Schlichthörl, G.; Nozik, A. J.; Grätzel, M.; Frank, A. J. *J. Phys. Chem. B* **1997**, *101*, 2576−2582.
(21) Vetter, K. J. *Electrochemical Kinetics*; Academic Press: New York, 1967.
(22) Hauch, A.; Georg, A. *Electrochim. Acta* **2001**, *46*, 3457−3466.
(23) Royea, W. J.; Fajardo, A. M.; Lewis, N. S. *J. Phys. Chem. B* **1997**, *101*, 11152−11159.
(24) Marcus, R. A.; Sutin, N. *Biochim. Biophys. Acta* **1985**, *811*, 265−322.
(25) Marcus, R. A. *J. Phys. Chem.* **1991**, *95*, 2010−2013.
(26) Vanmaekelbergh, D.; de Jongh, P. E. *J. Phys. Chem. B* **1999**, *103*, 747−750.
(27) Under this condition, the steady-state concentration of dye holes ($[d^+]$) could be significantly different from its thermodynamic equilibrium value ($[d^+]_{eq}$) in the dark. However, the concentration of the excited state of the dye is still assumed to be small compared to $[d]_0$.
(28) Gerischer, H. Semiconductor Photoelectrochemistry. In *Physical Chemistry: An Advanced Treatise*; Eyring, H., Henderson, D., Yost, W., Eds.; Academic: New York, 1970; Vol. 9A, pp 463−542.
(29) Memming, R. Electrochemistry II. In *Topics in Current Chemistry*; Stickham, E., Ed.; Springer-Verlag: New York, 1978; Vol. 143, pp 79−112.
(30) Tan, M. X.; Laibinis, P. E.; Nguyen, S. T.; Kesselman, J. M.; Stanton, C. E.; Lewis, N. S. *Prog. Inorg. Chem.* **1994**, *33*, 21−144.
(31) Albery, W. J.; Bartlett, P. N. *J. Electrochem. Soc.* **1984**, *131*, 315−325.
(32) Zaban, A.; Meier, A.; Gregg, B. A. *J. Phys. Chem. B* **1997**, *101*, 7985−7990.
(33) Schlichthörl, G.; Huang, S. Y.; Sprague, J.; Frank, A. J. *J. Phys. Chem. B* **1997**, *101*, 8141−8155.
(34) Kuciauskas, D.; Freund, M. S.; Gray, H. B.; Winkler, J. R.; Lewis, N. S. *J. Phys. Chem. B* **2001**, *105*, 392−403.
(35) Tachibana, Y.; Haque, S.; Mercer, I.; Moser, J.; Klug, D.; Durrant, J. *J. Phys. Chem. B* **2001**, *105*, 7424−7431.
(36) Lee, J.-J.; Coia, G. M.; Lewis, N. S. *J. Phys. Chem. B*, **2004**, *108*, 5282.
(37) Fitzmaurice, D. J.; Frei, H. *Langmuir* **1991**, *7*, 1129−1137.
(38) Kambili, A.; Walker, A.; Qiu, F.; Fisher, A.; Savin, A.; Peter, L. *Physica E* **2002**, *14*, 203−209.
(39) Skinner, D. E.; Colombo, D. P.; Cavaleri, J. J.; Bowman, R. M. *J. Phys. Chem.* **1995**, *99*, 7853−7856.
(40) Colombo, D. P.; Bowman, R. M. *J. Phys. Chem.* **1996**, *100*, 18445−18449.
(41) Rothenberger, G.; Fitzmaurice, D.; Grätzel, M. *J. Phys. Chem.* **1992**, *96*, 5983−5986.
(42) Peter, L. M.; Duffy, N. W.; Wang, R. L.; Wijayantha, K. G. U. *J. Electroanal. Chem.* **2002**, *524*, 127−136.
(43) Kopidakis, N.; Schiff, E.; Park, N.; van de Lagemaat, J.; Frank, A. *J. Phys. Chem. B* **2000**, *104*, 3930−3936.
(44) Shreve, G. A.; Lewis, N. S. *J. Electrochem. Soc.* **1995**, *142*, 112−119.